PARALLEL MORPHOLOGICAL CLASSIFICATION OF HYPERSPECTRAL IMAGERY USING EXTENDED OPENING AND CLOSING BY RECONSTRUCTION OPERATIONS

Antonio Plaza and Javier Plaza

Department of Technology of Computers and Communications, University of Extremadura
Avda. de la Universidad s/n, E-10071 Cáceres, Spain

ABSTRACT

Hyperspectral image processing has been a very active area in remote sensing and other application domains in recent years. Despite the availability of a wide range of advanced processing techniques for hyperspectral data analysis, many techniques for hyperspectral data classification are based on the consideration of spectral information separately from spatial information information, and thus the two types of information are not treated simultaneously. In this paper, we develop a new technique for joint spatial-spectral classification of hyperspectral image data which makes use of opening and closing by reconstruction, a kind of mathematical morphology operations which are extended here to hyperspectral images. A high performance parallel implementation of the proposed technique is also developed to satisfy time-critical constraints in remote sensing applications, using NASA's Thunderhead Beowulf cluster computer for demonstration purposes.

Index Terms— Hyperspectral imaging, mathematical morphology, high performance computing.

1. INTRODUCTION

Many currently available techniques for hyperspectral image processing treat the data not as images, but as unordered listings of spectral measurements with no spatial arrangement. The importance of analyzing spatial and spectral patterns simultaneously has been identified as a desired goal by many scientists devoted to hyperspectral data analysis [1, 2]. This type of processing has been approached in the past from various points of view. For instance, techniques have discussed the refinement of results obtained by applying spectral-based techniques to multispectral images (with tens of spectral channels) through a second step based on spatial context. Such contextual classification, extended also to hyperspectral images, accounts for the tendency of certain ground cover classes to occur more frequently in some contexts than in others. This approach consists of two parts: the definition of a pixel neighborhood (surrounding each pixel) and the performance of a local operation so that the pixel may be changed into the label mostly represented in the window that defines the neighborhood. This operation separates spatial from spectral information, and thus the two types of information are not treated simultaneously.

In previous work, we have developed extended versions of classic morphological operations [3] for hyperspectral scenes which integrate the spatial and spectral information [4]. Our extended morphological operations make use of a vector-based approach in which each pixel vector in the scene is ordered according to its spectral distance to other neighboring pixel vectors in the N-dimensional data set. Based on the ordering relation defined above, we can define extended erosion and dilation operations, which respectively select the pixel which is most spectrally similar and the pixel vector which is most spectrally distinct to its neighboring pixels. In order to avoid changing the size and shape of the features in the image, a desirable feature for spatial/spectral filtering, extended morphological opening and closing operations have also been defined, respectively, as extended erosion followed by extended dilation, and extended dilation followed by extended erosion [4]. It should be noted that all extended operators introduced so far are not reconstruction-based [3]. With morphological operations, it is highly desirable that the image features are either completely retained or completely removed in accordance with the size and shape of the structuring element, thus allowing one to perform most accurate classification based on spatial/spectral content.

In this paper, we develop a new parallel algorithm for thematic classification of hyperspectral images which has been specifically developed to be efficiently executed on massively parallel computing platforms. Parallelism is introduced as an effective approach to deal with the computational cost of morphological operations [5]. The algorithm integrates spatial and spectral information by making use of extended opening and closing by reconstruction operations, and then uses a parallel neural classifier. The paper is structured as follows. Section 2 presents the proposed framework to extend morphological opening and closing by reconstruction operations to hyperspectral images. Section 3 describes the parallel implementations. Section 4 provides an experimental validation of the proposed technique using a hyperspectral data set with extensive ground-truth. This section also includes performance results on NASA's Thunderhead massively parallel cluster. Section 5 concludes with some remarks.

978-1-4244-2808-3/08/$25.00 ©2008 IEEE

2. EXTENDED MORPHOLOGICAL OPERATIONS

In order to introduce opening and closing by reconstruction operations for a hyperspectral image $\mathbf{F}$, we adopt a distance-based technique which utilizes a cumulative distance between one particular pixel vector $\mathbf{F}(x, y)$, where (x, y) indicates the spatial coordinates, and all the pixel vectors in the spatial neighborhood given by a SE denoted by K as follows [4]:

$$C_K(\mathbf{F}(x,y)) = \sum_{(s,t)\in K} \mathrm{SAD}(\mathbf{F}(x,y), \mathbf{F}(s,t)), \qquad (1)$$

where SAD is the spectral angle distance. As a result, $C_K(\mathbf{F}(x, y))$ is given by the sum of SAD scores between $\mathbf{F}(x, y)$ and every other pixel vector in the K-neighborhood. At this point, we need to define a maximum and an minimum given an arbitrary set of vectors $\mathbf{S} = \{\mathbf{v}_1, \mathbf{v}_2, \cdots, \mathbf{v}_p\}$, where k is the number of vectors in the set. This is done by computing $C_K(\mathbf{S}) = \{C_K(\mathbf{v}_1), C_K(\mathbf{v}_2), \cdots, C_K(\mathbf{v}_k)\}$ and selecting $\mathbf{v}_i$ such that $C_K(\mathbf{v}_i)$ is the minimum of $C_K(\mathbf{S})$, with $1 \leq i \leq k$. In similar fashion, we can select $\mathbf{v}_j$ such that $C_K(\mathbf{v}_j)$ is the maximum of $C_K(\mathbf{S})$, with $1 \leq j \leq p$. Based on the definitions above, the extended erosion $\mathbf{F} \ominus K$ consists of selecting the K-neighborhood pixel vector that produces the minimum C_K value as follows [4]:

$$(\mathbf{F} \ominus K)(x,y) = argmin_{(s,t)\in K}\{C_K(\mathbf{F}(x+s, y+t)\}. \quad (2)$$

On the other hand, the extended dilation $\mathbf{F} \oplus K$ selects the K-neighborhood pixel that produces the maximum value for C_K as follows [4]:

$$(\mathbf{F} \oplus K)(x,y) = argmax_{(s,t)\in K}\{C_K(\mathbf{F}(x-s, y-t)\}. \quad (3)$$

Based on the above operations, extended morphological opening and closing can be simply defined, respectively, as follows: $(\mathbf{F} \circ K)(x, y) = [(\mathbf{F} \ominus K) \oplus K](x, y)$, i.e., erosion followed by dilation, and $(\mathbf{F} \bullet K)(x, y) = [(\mathbf{F} \oplus K) \ominus K](x, y)$, i.e., dilation followed by erosion [4]. Again, these operations are not reconstruction-based. Our extended opening by reconstruction for each local pixel $\mathbf{F}(x, y)$ is given by the following expression:

$$(\mathbf{F} \circ K)^t(x,y) = min_{t\leq 1}\{\delta_K^t(\mathbf{F} \circ K|\mathbf{F})(x,y)\}, \qquad (4)$$

where $\delta_K^t(\mathbf{F} \circ K|\mathbf{F})(x, y) = \delta_B\delta_B \cdots \delta_B(\mathbf{F} \circ K|\mathbf{F})(x, y)$, i.e., the operator δ_B is applied t times, and $\delta_B(\mathbf{F} \circ K|\mathbf{F})(x, y) = min\{[(\mathbf{F} \circ K) \oplus K](x, y), \mathbf{F}(x, y)\}$. Similarly, the extended closing by reconstruction for each local pixel $\mathbf{F}(x, y)$ is calculated as follows:

$$(\mathbf{F} \bullet K)^t(x,y) = min_{t\leq 1}\{\delta_K^t(\mathbf{F} \bullet K|\mathbf{F})(x,y)\}, \qquad (5)$$

where $\delta_K^t(\mathbf{F} \bullet K|\mathbf{F})(x, y) = \delta_B\delta_B \cdots \delta_B(\mathbf{F} \bullet K|\mathbf{F})(x, y)$, i.e., the operator δ_B is applied t times, and $\delta_B(\mathbf{F} \bullet K|\mathbf{F})(x, y) = min\{[(\mathbf{F} \bullet K) \ominus K](x, y), \mathbf{F}(x, y)\}$.

With the extended opening and closing by reconstruction operations in mind, we have developed a spatial-spectral feature extraction algorithm that replaces each hyperspectral image pixel by a so-called extended morphological profile which integrates the spatial and the spectral information. The algorithm consists of the following steps:

1. Compute the derivative of the extended opening profile as: $\boldsymbol{p}_t^\circ = \{\mathrm{SAD}[(\mathbf{F} \circ K)^\lambda(x, y), (\mathbf{F} \circ K)^{\lambda-1}(x, y)]\}$, with $\lambda = \{1, 2, \cdots, t\}$. Here, $\mathbf{F}(x, y) = (\mathbf{F} \circ K)^0(x, y)$ for $\lambda = 0$.

2. Compute the derivative of the extended closing profile as: $\boldsymbol{p}_t^\bullet = \{\mathrm{SAD}[(\mathbf{F} \bullet K)^\lambda(x, y), (\mathbf{F} \bullet K)^{\lambda-1}(x, y)]\}$, with $\lambda = \{1, 2, \cdots, t\}$. Here, $\mathbf{F}(x, y) = (\mathbf{F} \bullet K)^0(x, y)$ for $\lambda = 0$.

3. Form a $(2t-1)$-dimensional profile for each local pixel $\mathbf{F}(x, y)$ by combining the derivatives of the extended opening and closing profiles as follows: $\mathrm{MP}(x, y) = \{\boldsymbol{p}_t^\circ(x, y), \boldsymbol{p}_t^\bullet(x, y)\}$. The resulting profile can be seen as a spatial-spectral feature vector on which a subsequent classification procedure may be applied. In this work, we have resorted to a parallel multi-layer perceptron (MLP) neural network classifier, as described in the following subsection.

3. PARALLEL IMPLEMENTATIONS

In order to exploit parallelism as much as possible, we have adopted a standard master-slave parallel processing paradigm combined with spatial-domain partitioning for the parallel implementation of morphological operations [5]. Spatial-domain partitioning subdivides the original data volume into slabs which are made up of (contiguous) pixel vector rows, thus retaining the full spectral information associated to each pixel vector at the same processor. In this type of processing, additional inter-processor communications will be required when the SE-based computation needs to be split amongst several different processing when the SE is centered around a pixel vector located in the border of one of the local partitions resulting after spatial-domain decomposition, as illustrated by Fig. 1(a). In this case, the computations for the pixel vector at spatial coordinates $(5, 3)$ in the original image, denoted by $\mathbf{F}(5, 3)$, will need to originate from two processing elements since this pixel becomes a border pixel after spatial-domain partitioning. As a result, a communication overhead involving three N-dimensional pixel vectors (located in partition #2) is required in order to complete the SE-based computation for the pixel vector $\mathbf{F}(5, 3)$ in partition #1. However, if an overlap border is carefully added to partition #1 (consisting of the entire first row of pixels allocated to partition #2), as illustrated in Fig. 1(b), then boundary data no longer need to be exchanged between neighboring processors.

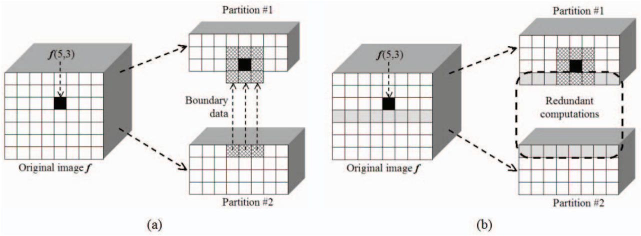

Fig. 1. (a) 3×3-pixel morphological computation split among two processing elements. (b) Introduction of an overlap border to minimize inter-processor communication in a 3×3-pixel computation.

With the above parallel framework in mind, three different strategies have been tested for efficient implementation of morphological operations. In all cases, the master processor first partitions the data in the spatial domain and distributes the partitions to the worker processors as described in Fig. 1(b). Once the workers finalize processing their parts, the master gathers the individual $(2t-1)$-dimensional profiles provided by the workers and merges them into a new data cube with $2t-1$ components. This approach requires minimal coordination between the master and the workers, namely, at the beginning and ending of the parallel process, although it is subject to a redundant computation overhead introduced by the overlap borders used by the proposed data partitioning strategy. In order to analyze this issue in more detail, three different implementation strategies have been tested:

1. The first one (called MP-1) implements a standard data partitioning operation followed by overlap border communication for every hyperspectral pixel vector, thus communicating small sets of pixels very often.

2. The second one (called MP-2) implements a standard data partitioning operation followed by a special overlap communication which sends all border data beforehand, but only once.

3. The third one (called MP-3) implements a special data partitioning operation that also sends out the overlap border data as part of the scatter operation itself.

Once morphological features have been extracted, a robust classification using a parallel MLP neural network with backpropagation learning follows (see additional details in [6]). The parallel classifier is trained with selected features from the previous morphological feature extraction stage. Two different partitioning strategies have been tested:

1. The first one (called *exemplar partitioning*) partitions the training pattern data set so that each processor determines the weight changes for a disjoint subset of the training population and then changes are combined and applied to the neural network at the end of each epoch.

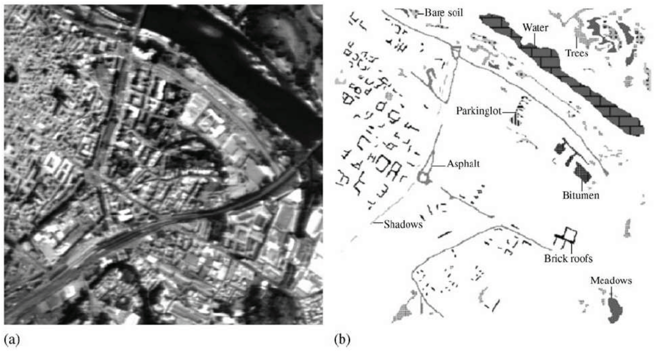

Fig. 2. (a) Band at 639 nm of a DAIS 7915 hyperspectral image over Pavia, Italy; (b) Ground-truth classes.

2. The second one (called *hybrid partitioning*) partitions the hidden layer of the neural network using *neuronal-level* parallelism, while parallelization of the weight connections adopts *synaptic-level* parallelism.

4. EXPERIMENTAL RESULTS

The classification accuracy of the parallel classification algorithm (comprising parallel morphological feature extraction followed by parallel neural classification) has been tested using a hyperspectral data set collected by the DAIS 7915 sensor over an area comprising several urban features in Pavia, Italy, in which integration of spatial and spectral features is crucial. Fig. 2(a) shows the band at 639 nm of the considered hyperspectral scene, while Fig. 2(b) shows the ground-truth map with nine mutually-exclusive classes. The data set comprises 400×400 pixels, each with spatial resolution of 5 meters, and a total of 40 spectral bands.

In order to test the accuracy of the proposed parallel morphological/neural classifier, a random sample of less than 2% of the ground truth pixels was used for training. Table 1 shows the individual and overall classification accuracies obtained for each class using standard [4] and extended opening/closing and reconstruction-based operations (with $t=5$) for feature extraction. The table also includes the accuracies obtained using the full spectral information and principal component transform (PCT)-reduced features [2] as input to the MLP neural classifier. As shown by Table 1, the accuracies were higher when reconstruction-based operations were used due to a better use of spatial-spectral information.

On the other hand, a 256-processor Beowulf cluster (Thunderhead) at NASA's Goddard Space Flight Center[1] has been used to validate the efficiency of the proposed parallel algorithms. The Thunderhead cluster is currently composed of 268 dual 2.4 Ghz Intel 4 Xeon nodes, each with 1 GB of memory and 80 GB of hard disk. Table 2 reports the processing times (in seconds) and speedups achieved by

[1] http://thunderhead.gsfc.nasa.gov

Table 1. Number of training/test samples and classification accuracies (%) achieved by different classifiers.

Ground-truth class	Training samples	Test samples	Spectral information	PCT-based features	Standard opening/closing	Reconstruction-based opening/closing
Water	114	4176	87.30	91.90	92.55	100.00
Trees	101	2444	94.64	93.21	95.61	98.72
Asphalt	85	1614	97,79	95.43	97.33	98.88
Parking lot	59	229	83.82	94.28	94.87	71.77
Bitumen	65	629	86.11	86.38	90.45	98.68
Brick roofs	106	2132	83.69	84.21	92.12	99.37
Meadow	62	1183	88.88	89.45	88.95	92.61
Bare soil	74	1401	79.85	88.24	92.06	95.11
Shadows	52	181	89.64	93.45	94.11	96.19
Overall accuracy	–	–	88.65	86.21	92.53	96.16

Table 2. Processing times in seconds and speedups (in the parentheses) on NASA's Thunderhead cluster.

Processors	**4**	**16**	**36**	**64**	**100**	**144**	**196**	**256**
MP-1	1177 (1.8)	339 (6.5)	146 (15.0)	81 (27.2)	53 (41.5)	42 (52.4)	37 (59.5)	36 (61.2)
MP-2	797 (2.5)	203 (10.0)	79 (25.8)	39 (52.3)	23 (88.73)	17 (120.0)	13 (157.0)	10 (204.1)
MP-3	826 (2.4)	215 (9.5)	88 (23.3)	45 (45.7)	27 (76.2)	20 ()	16 (102.9)	12 (171.5)
Processors	**2**	**4**	**8**	**16**	**32**	**64**	**128**	**256**
Exemplar	1041 (1.9)	414 (4.8)	248 (8.1)	174 (11.5)	142 (14.1)	99 (20.2)	120 (16.7)	120 (16.7)
Hybrid	973 (1.6)	458 (3.5)	222 (7.2)	114 (14.0)	55 (29.2)	27 (59.5)	15 (107.1)	7 (229.5)

multi-processor runs with regards to single-processor runs of the parallel algorithm on Thunderhead. The table reveals that MP-2 partitioning and hybrid neural parallelism respectively provided the best results for each stage. Using 256 Thunderhead processors, the parallel classifier (based on MP-2 and hybrid neural parallelism) was able to provide a highly accurate classification of the considered hyperspectral scene in only 17 seconds, which represents a significant improvement over the serial implementation, which can take up to several minutes for the considered problem size.

From the experimental results described in this section, an important final observation is noteworthy: contrary to the common perception that spatial-spectral algorithms involve more complex operations than traditional, spectral-based techniques, results in this paper indicate that spatial-spectral techniques, when carefully designed and implemented, can indeed be more *pleasingly parallel* than spectral-based techniques, mainly because they can reduce sequential computations at the master and only involve minimal communication between the parallel tasks, namely, at the beginning and ending of such tasks.

5. CONCLUSIONS

In this paper, we have discussed the role of joint spatial-spectral information (via specialized morphological processing using extended opening and closing by reconstruction operations) in the analysis of hyperspectral images. Our experimental assessment, conducted both from the viewpoint of classification accuracy and parallel performance, revealed important considerations about the properties and nature of the proposed algorithms. Specifically, performance results (measured on the Thunderhead system at NASA's Goddard Space Flight Center) indicate that the proposed parallel techniques were able to provide adequate results in both the quality of the solutions and the time to obtain them. As future work, we plan to implement the parallel spatial-spectral algorithms discussed in this work on alternative high performance computing architectures, such field programmable gate arrays (FPGAs) and graphic processing units (GPUs). These platforms may allow us to fully accomplish the challenge of real-time classification of hyperspectral image data.

6. REFERENCES

[1] A. Plaza, J. A. Benediktsson, J. Boardman, J. Brazile, L. Bruzzone, G. Camps-Valls, J. Chanussot, M. Fauvel, P. Gamba, J.A. Gualtieri, M. Marconcini, J. C. Tilton and G. Trianni, "Recent advances in techniques for hyperspectral image processing," *Remote Sensing of Environment*, in press, 2008.

[2] D. A. Landgrebe, *Signal theory methods in multispectral remote sensing*, Wiley: New York, 2003.

[3] P. Soille, *Morphological image analysis: principles and applications*. Springer: Berlin, 2003.

[4] A. Plaza, P. Martinez, J. Plaza and R. Perez, "Dimensionality reduction and classification of hyperspectral image data using sequences of extended morphological transformations," *IEEE Trans. Geosci. Remote Sensing*, vol. 43, pp. 466–479, 2005.

[5] A. Plaza, D. Valencia, J. Plaza and P. Martinez, "Commodity cluster-based parallel processing of hyperspectral imagery," *Journal of Parallel and Distributed Computing*, vol. 66, pp. 345–358, 2006.

[6] J. Plaza, R. Perez, A. Plaza, P. Martinez and D. Valencia, "Parallel morphological/neural processing of hyperspectral images using heterogeneous and homogeneous platforms," *Cluster computing*, vol. 11, pp. 17–32, 2008.